Available online at www.sciencedirect.com
ScienceDirect
Geochimica et Cosmochimica Acta 70 (2006) 4579–4599
Geochimica
www.elsevier.com/locate/gca

Surface chemistry of kaolinite and Na-montmorillonite in aqueous electrolyte solutions at 25 and 60 °C: Experimental and modeling study

E. Tertre [a,b,*], S. Castet [a], G. Berger [a], M. Loubet [a], E. Giffaut [b]

[a] LMTG (Université Toulouse III, UMR CNRS 5563), 14 av. E. Belin, 31400 Toulouse, France
[b] ANDRA, Parc de la Croix Blanche, 92298 Châtenay-Malabry cedex, France

Received 19 December 2005; accepted in revised form 11 July 2006

Abstract

The aqueous interfacial chemistry of kaolinite and Na-montmorillonite samples was investigated by potentiometric measurements using acid/base continuous titrations and batch experiments at 25 and 60 °C. Using the batch experimental method, a continuous drift of pH was observed reflecting the mineral dissolution. Consequently, the continuous titration method appears to be the best way of studying solid surface reactions. For each clay mineral, the net proton surface excess/consumption was calculated as a function of pH and ionic strength (0.025, 0.1 and 0.5 M). At 25 °C, and according to the literature data, the pH corresponding to zero net proton consumption for montmorillonite appears to depend on ionic strength, whereas the value for kaolinite is constant and close to 5. Similar results are obtained at 60 °C, which suggests that the point of zero net proton consumption for clay minerals does not depend on temperature, at least up to 60 °C. On the other hand, the temperature rise induces a slight increase of the net proton surface excess. Finally, the diffuse double layer formalism (DDLM) is used to model the experimental data. The model involves two processes: the protonation/deprotonation of two types of edge sites (aluminol and silanol) and H^+/Na^+ exchange reactions on basal surfaces, while a tiny proportion of the negative structural charge remains uncompensated. This last process maintains a negative surface potential whatever the pH of the solution, which is in agreement with electrokinetic data.

1. Introduction

The migration of toxic elements through soils and rocks is largely influenced by sorption processes at the solid-solution interface. Among the more common minerals, clays have a very strong retention capacity due to (i) their high surface area and (ii) the property of these minerals to show a permanent negative charge within the structure at the same time as a variable charge at the particle edges. This latter feature is now well recognized, and numerous studies have focused on measuring and modeling the net surface proton excess of clay minerals (smectites: Wanner et al., 1994; Baeyens and Bradbury, 1997; Avena and De Pauli, 1998; Kraepiel et al., 1998; Tombacz et al., 2004; Tournassat et al., 2004a; on kaolinites: Schindler et al., 1987; Brady and Walther, 1992; Wieland and Stumm, 1992; Schroth and Sposito, 1997; Angove et al., 1998; Huertas et al., 1998; Sverjensky and Sahai, 1998; Ward and Brady, 1998; Fournier, 2002; illites: Du et al., 1997; Sinitsyn et al., 2000). Nevertheless, despite these numerous studies, experimental results are still disparate. As an example, the pH_{PZNPC} (point of zero net proton charge) for kaolinite varies from 4 (Schindler et al., 1987) to 7.5 (Wieland and Stumm, 1992). One reason for these discrepancies could be linked to contrasting experimental methods: some authors used continuous potentiometric titrations with short equilibration times (Brady and Walther, 1992; Wieland and Stumm, 1992; Huertas et al., 1998; Ward and Brady, 1998), while others used potentiometric measurements in batch experiments over long equilibration times (Baeyens and Bradbury, 1997; Tournassat et al.,

* Corresponding author.
E-mail address: Emmanuel.Tertre@univ-lille1.fr (E. Tertre).

0016-7037/$ - see front matter © 2006 Elsevier Inc. All rights reserved.
doi:10.1016/j.gca.2006.07.017

2004a). These two methods are compared in the present study to find out which one is better adapted to study surface reactions.

On the other hand, the influence of ionic strength on the surface properties of clay minerals has not been deeply studied. In the case of montmorillonite, only a few authors (Avena and De Pauli, 1998; Tombacz et al., 2004) have proposed a model that reproduces the titration data obtained at 25 °C for different ionic strengths. Huertas et al. (1998) interpret titration data obtained at three ionic strengths for kaolinite at room temperature, but the pK_a values used for edge sites and the corresponding densities vary with ionic strength.

Lastly, no titration data are currently available for 2:1 clay minerals at elevated temperatures. For kaolinite, Angove et al. (1998) and Ward and Brady (1998) report a slight increase of the proton surface charge with a rise in temperature up to 70 or 60 °C, respectively. As for simple oxides, literature data generally show that the pH_{PZNPC} of these minerals decreases slightly with increasing temperature (Blesa et al., 1984; Brady, 1992, 1994; Mustapha et al., 1998; Sverjensky and Sahai, 1998; Machesky et al., 2001). However, these results must be taken with caution given the scattering of the values proposed at 25 °C.

Therefore, the second objective of the present study was to provide a set of consistent titration data as a function of both temperature and ionic strength, and to compare the results obtained with two very different clays: kaolinite and montmorillonite. Indeed, kaolinites have a very low permanent charge (CEC between 5 and 15 meq/100 g), whereas montmorillonites, which exhibit numerous isomorphic substitutions, have a high permanent charge ($80 < CEC < 120$ meq/100 g) (Bouchet et al., 2000). In this way, we investigated the influence of the structural negative charge of the clays on their net proton surface excess.

Potentiometric measurements were carried out at 25 and 60 °C, at three ionic strengths ($I = 0.025$, 0.1 and 0.5 M) and using both continuous titrations and batch experiments. The data were then interpreted using the diffuse double layer model (DDLM) and the computer code FITEQL 3.2 (Herbelin and Westall, 1996).

2. Previous studies

Nowadays, there are still rather few studies dedicated to the surface chemistry of clays mineral, particularly their acid/base properties. Kaolinite, which exhibits the simplest structure, is among the most studied of these minerals (Schindler et al., 1987; Brady and Walther, 1992; Wieland and Stumm, 1992; Schroth and Sposito, 1997; Angove et al., 1998; Huertas et al., 1998; Sverjensky and Sahai, 1998; Ward and Brady, 1998; Fournier, 2002). Nevertheless, the data reported in these studies are often disparate. This disagreement concerns the values of the net proton consumption as well as the point of zero net proton consumption (i.e. pH_{PZNPC}). However, the discrepancy can be reduced by taking account of the contribution of solid dissolution, as shown by Ganor et al. (2003).

The surface chemistry of montmorillonite is less well documented (Baeyens and Bradbury, 1997; Bradbury and Baeyens, 1997; Avena and De Pauli, 1998; Tombacz and Szekeres, 2004; Tombacz et al., 2004; Tournassat et al., 2004a,b) and, as in the case of kaolinite, there seems to be a lack of any consensus about the values of the net proton surface excess for this mineral.

Similarly, titrations of clays and oxides at temperatures higher than 25 °C are not documented in detail. Angove et al. (1998) show that, for a fixed pH, the net proton consumption of kaolinite increases slightly when temperature increases from 10 to 70 °C. Ward and Brady (1998) also concluded that increasing the temperature to 60 °C leads to an increase of the kaolinite proton surface charge between pH 4 and 9. For simple oxides, studies at temperature higher than 25 °C are also rare. Generally, experiments show that the pH_{PZNPC} of oxides decreases slightly with increasing temperature. For example, Brady (1994) shows that the pH_{PZNPC} of γ-Al_2O_3 decreases from 6.45 at 25 °C to 6.32 at 60 °C. However, all these considerations about the temperature dependence of the surface charge should be treated with great prudence given the dispersion of values reported at 25 °C for any single mineral. For montmorillonite, which differs from kaolinite and oxides in having a significant and high negative structural charge, no data are currently available at elevated temperature.

Whatever the mineral and the temperature, the comparison of previous data is complicated by the fact that the solid phases are not always exactly the same. This applies also to the solid purification procedures, the experimental protocols and/or the approach used to treat and interpret the results.

This point is particularly well developed in the recent review by Duc et al. (2005a). The composition of the solid phase and the procedure used for its purification can evidently lead to scattered results. On the other hand, the influence of the experimental protocol on the reliability of the data is not so clear. Three techniques are usually applied to obtain the proton surface charge of a solid phase. The most frequently used is continuous titration, which consists of measuring the pH of a suspension after the addition of an aliquot of titrant. This method was often used for simple oxides (Bérubé and Debruyn, 1968; Abendroth, 1970; Huang and Stumm, 1973; Kita et al., 1981; Brady and Walther, 1992; Brady, 1994) and was sometimes applied to study the surface chemistry of clays (Ward and Brady, 1998; Huertas et al., 1998; Avena and De Pauli, 1998). The short duration of the experiment minimizes concomitant reactions such as mineral dissolution. However, the rapidity of this method can also raise questions about the achievement of surface reaction equilibrium. The second technique is batch titration, which involves several experiments carried out on various time scales, each providing a unique potential value. One of the obvious drawbacks of this method is the large number

of runs required to cover a wide range of pH. In the case of long equilibration times, we can add a significant contribution from solid dissolution. Finally, the third method is back titration (Schulthess and Sparks, 1986; Baeyens and Bradbury, 1997; Tournassat et al., 2004a), which is carried out in two steps: a batch experiment followed by solid/solution separation and a back titration of the remaining solution to determine the concentration of aqueous hydrolyzed species. This last technique does not appear to offer any additional advantages compared to the others, insofar as any method can be adapted to measure the concentrations of aqueous species and thus quantify hydrolysis reactions. Therefore, in the present study, we compare the results obtained with the continuous and batch titration methods.

The only common feature in the literature data—at least at 25 °C—is that, contrary to simple oxides, the net proton consumption versus pH curves obtained at different ionic strengths, in most cases, do not intersect at a single point, i.e. the point of zero proton charge. Indeed, these curves are almost superimposed for kaolinite (Huertas et al., 1998; Ganor et al., 2003) and parallel for montmorillonite (Avena and De Pauli, 1998; Tombacz et al., 2004). The particular behavior of clays, compared with simple oxides, is linked to the negative permanent charge of these minerals, which is higher for montmorillonite than for kaolinite. Furthermore, electrokinetic measurements on clays (Hussain et al., 1996; Sondi et al., 1997; Avena and De Pauli, 1998; Thomas et al., 1999; Missana and Adell, 2000; Hu and Liu, 2003) show systematically negative potential values whatever the pH and the ionic strength investigated, even for kaolinite which has the lowest CEC. Nevertheless, only few authors (Avena and De Pauli, 1998; Kraepiel et al., 1998; Tombacz et al., 2004) have used these observations at 25 °C to develop models for the clay/solution interface. These authors take into account both the negative structural charge and the variable charge at the edges, while maintaining a negative surface potential irrespective of pH. In this way, such models are effectively able to fit the titration and electrokinetic data at different ionic strengths. These different models are described, discussed and compared in Section 6 below, to provide a basis for a surface speciation model capable of reproducing the data obtained for both kaolinite and montmorillonite as a function of ionic strength and temperature.

3. Materials and methods

3.1. Materials

The kaolinite used in this study is the St Austell kaolinite from the UK, distributed under the trade name SUPREME and supplied by English China Clays. Its specific surface area, determined by the BET method (N_2 adsorption), was found to be 10 m^2/g. The structural formula of this kaolinite was reported to be: $Al_2Si_2O_5(OH)_4$ (Coppin et al., 2002). A CEC of 3.7 meq/100 g was determined by Bauer (1997), according to the Meir and Kahr method (1999).

The montmorillonite was extracted from the bentonite MX-80, which was supplied by the Bureau de Recherches Géologiques et Minières in France. The protocol of extraction of the clay fraction is detailed in Tertre et al. (2005). The resulting smectite corresponds to a sodi-calcic montmorillonite with the following structural formula (Sauzeat et al., 2002):

$$(Si_{3.98}Al_{0.02})(Al_{1.55}Mg_{0.28}Fe^{III}_{0.09}Fe^{II}_{0.08})Na_{0.18}Ca_{0.10}O_{10}(OH)_2$$

This montmorillonite is then Na saturated in two stages : (i) five washings with 1 mol/L NaCl solutions to transform the montmorillonite into the Na^+ form and (ii) successive washings of the clay with 0.025 M $NaClO_4$ solutions until equilibration between the solid and the electrolyte solution was achieved. The XRD diagram of the final solid shows a d_{001} at 12.49 Å. The BET method (N_2 adsorption) yields a specific surface area for this mineral of 24 m^2/g. A CEC of 87.5 ± 2 meq/100 g, was measured by the cobalt hexamine method (Sauzeat et al., 2002). This value corresponds however to a hydrated solid (11%wt), which implies a CEC value of 97 meq/100 g for the dehydrated montmorillonite in good agreement with the theoretical CEC of 102 meq/100 g. Tournassat et al. (2004a) have proposed a slightly modified formula for the same material, with a CEC of 76 meq/100 g reflecting a higher proportion of ferric iron. These authors suggest that the treatments of the solid phase with DCB (dithionate–citrate–bicarbonate) followed by H_2O_2 could have changed the Fe(II)/Fe(III) ratio. Since the solid phase used in our study was neither heated nor treated with oxidizing agents, we only take into account the experimental value proposed by Sauzeat et al. (2002).

For practical reasons, we chose to use a grain-size fraction coarser than 0.2 μm for both the clays. This fraction was used to prepare three stock suspensions of each clay mineral in $NaClO_4$ solutions, with a solid/solution ratio of 2.5 g L^{-1} and at three ionic strengths (0.025, 0.1 and 0.5 M). These initial suspensions were stored at 25 °C. All the solutions were prepared with deionized water (Milli-Q Reagent Water System from Millipore Corporation) with a resistivity higher than 18 MΩ cm^{-1}.

3.2. Experimental protocols

3.2.1. Continuous titrations

The reversibility of the studied surface reactions is a crucial point to check in order to apply a thermodynamic model and acquire the corresponding thermodynamic constants. Previous experimental works on the surface chemistry of montmorillonite (Tombacz et al., 2004; Tombacz and Szekeres, 2004) have mentioned a hysteresis when successive forward and backward titrations are carried out. More recently, Duc et al. (2005b) performed a systematic analysis of the different parameters that might interfere

during such experiments and recommended a framework for optimal experimental conditions in order to (i) minimize the hysteresis and (ii) get a better reproducibility and accuracy of the measurements. According to this latter study, the solid used in the present work was wet and freshly synthesized (less than 3 months old); the titrations were carried out under pure N_2 and the potentials recorded within short time intervals.

Preliminary experiments have been performed where the titrations were carried out in three stages: the suspension was first titrated with a 0.1 M $HClO_4$ solution from near neutral to acidic pH, the same suspension was then titrated with a 0.01 M NaOH solution up to pH ≈ 9 and finally back titrated down to pH ≈ 4. Apart for the first downward run, the two final titrations gave similar results, within the experimental reproducibility and therefore demonstrated a reversible process. These results are in agreement with those from Tombacz et al. (2004) and Tombacz and Szekeres (2004). Consequently, and according to the recommendations of Duc et al. (2005b), the second step was only considered in the subsequent titrations, which were carried out as follows. Thirty milliliters of suspension was titrated in a polyethylene vessel with the temperature regulated at 25 or 60 °C by means of water circulation. Before the titration, 100 μL of $HClO_4$ 0.1 M (Prolabo, RP Normapur) was added to the suspension to obtain a pH around 4. The sample was continuously stirred and purged with pure nitrogen gas during the whole experiment. The titration was started 2 h after a first stage of homogenization under these conditions. The suspension was then titrated with incremental volumes (10–50 μL) of 0.01 M NaOH solution (Prolabo, RP Normapur) until the pH reached a value close to 10. The pH was recorded when the variation of the potential became less than 2 mV min^{-1}. Indeed, preliminary tests have shown that below this value, and particularly between pH 4 and 6, the mineral dissolution induces a slow but continuous potential drift. Thus, the parameters chosen for the continuous method allows minimizing the effects due to mineral dissolution. Generally speaking, the time required to reach a stable potential varied from 1 to 10 min, depending on the pH value, and the total duration of a titration never exceeded 5 h. The total amount of base added to the suspension was less than 5% of the initial volume, in order to minimize the dilution effect. This dilution factor is taken into account in the calculations presented below. The same protocol was used to titrate blank electrolyte solutions ($NaClO_4$) at each ionic strength and at each temperature. All the experiments were replicated three times to check the reproducibility of the method.

3.2.2. Batch experiments

The batch experiments were performed at the same temperatures and ionic strengths as the continuous titrations. They were carried out in PTFE containers, with about 6 mL of clay suspension. Variable volumes of $HClO_4$ or NaOH (Prolabo, RP Normapur) are added to the containers in order to cover a pH range from 4 to 9. The suspensions were purged with pure nitrogen gas for 2 h with continuous stirring. Then, the containers were sealed and stored in a oven regulated at 25 or 60 °C. Manual shaking of the containers was carried out several times a day during the experiment. Different equilibration times were tested: 24, 48 and 168 h. At the end of each run, the pH of the suspension was measured at the experimental temperature.

Table 1
Dissociation constants for H_2O, at 25 and 60 °C, used in the present study (from Tanger and Helgeson, 1997)

T (°C)	$\log K_{H_2O}$
25	−13.99
60	−12.92

For both methods, the pH was measured with a Mettler Toledo® (DG114) combined electrode. At $I = 0.025$ and 0.1 M, the electrode calibration was performed, on activity scale, with three buffer solutions (Hanna Instruments, pH 4.01, 6.86 and 9.18 at 25 °C). Activity coefficients for hydrogen and hydroxyl ions were calculated using the Bates–Guggenheim convention, according to the IUPAC recommendations (Buck et al., 2002). The concentrations of these ions were subsequently deduced from the dissociation constant of water at the considered temperature (Table 1) and the hydrogen and hydroxyl ion activity coefficients. For the experiments performed at $I = 0.5$ M, the electrode was calibrated on a concentration scale using $HClO_4/NaClO_4$ or $NaOH/NaClO_4$ solutions at the same ionic strength. The measured slopes differ by less than 5% from the theoretical slope of the Nernst law at the considered temperature. In this case, the H^+ and OH^- activity coefficients needed to calculate the corresponding pH and hydroxyl ion concentration were computed using the Davies equation.

4. Determination of the net proton surface excess/consumption

4.1. Blank experiments

Titrations of blank solutions were carried out to quantify the whole set of reactions which consume or release protons and which cannot be monitored during the experiments. These processes include possible reactions with the container walls or with impurities present in the sample, such as, for example, carbonate ions. We assume here that if such reactions are involved in the blank experiments, they occur to the same extent in the presence of a mineral. Thus, the quantification of such reactions allows us to subtract their effects from the suspension titration results. These processes can be quantified by the measured deviation from electroneutrality of the solution, denoted as ΔQ^{blank} (mol/L), and computed at each titration point according to Eq. (1)

$$\Delta Q^{blank}(\text{mol/L}) = C_a - C_b - [H^+] + [OH^-] \quad (1)$$

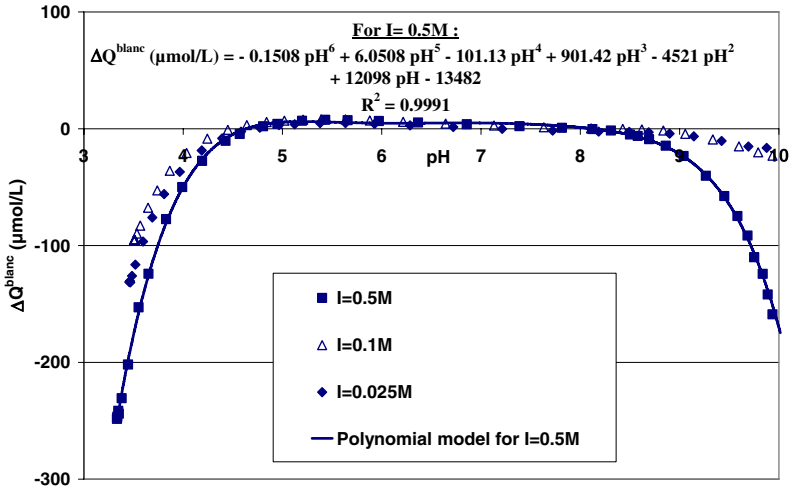

Fig. 1. Deviation from electroneutrality for blank experiments as a function of pH and ionic strength (experimental conditions: 25 °C, continuous titrations).

Where C_a and C_b are the concentrations of acid and base added (mol/L); $[H^+]$ and $[OH^-]$ are the aqueous concentrations of H^+ and OH^- (mol/L) derived from the electrode calibration.

The term ΔQ^{blank}, obtained from continuous titrations performed at 25 °C, is plotted in Fig. 1 as a function of pH and ionic strength. This plot shows that side reactions are only significant for pH < 4 and pH > 9, in agreement with the results reported by Shen et al. (1999). At 60 °C, the results are acceptable in the pH range 4–8. Similar conclusions can be drawn for results obtained with the batch method. Therefore, our experiments were restricted to the ranges of pH, 4–9 at 25 °C, and 4–8 at 60 °C. The values of ΔQ^{blank} versus pH were then fitted with a polynomial equation to correct the data obtained for the suspension under the same conditions of temperature and ionic strength. Such a fitting is illustrated in Fig. 1, for a run conducted at $I = 0.5$ M and 25 °C.

4.2. Suspensions

In the presence of a mineral, as in the case of blank experiments, we can compute the term $\Delta Q^{susp.}$ (Eq. (1)) at every point of the titration or for each batch experiment, and then correct it for side reactions by means of Eq. (2)

$$\Delta Q^{solid}(\text{mol/L}) = \Delta Q^{susp.} - \Delta Q^{blank}_{comp.} \quad (2)$$

In this equation, $\Delta Q^{blank}_{comp.}$ is the correction term computed from the polynomial equation previously described and ΔQ^{solid} can be defined as the deviation from electroneutrality due solely to the presence of the mineral. Fig. 2 illustrates the extent of this correction on the results obtained from continuous titration of the Na-montmorillonite at 25 °C and $I = 0.5$ M. In this plot, the uncorrected data correspond to the average of the three replicates and the associated error bars reflect the reproducibility of the

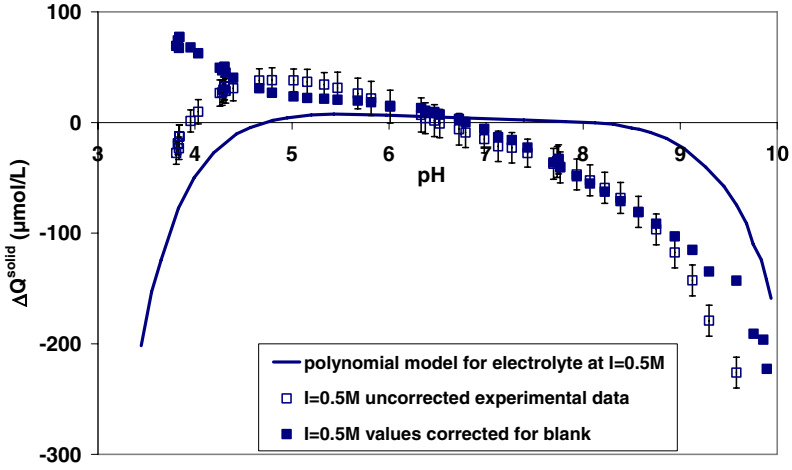

Fig. 2. Experimental data, as a function of pH, obtained from continuous titration of Na-montmorillonite at 25 °C and $I = 0.5$ M. Comparison between raw data and those corrected for blank.

experiments. This uncertainty is far higher than the error on the computed term $\Delta Q_{\text{comp.}}^{\text{blank}}$.

In simple cases, such as oxides where only proton adsorption/desorption processes are occurring, the term ΔQ^{solid} corresponds to the surface proton concentration and can be easily related to the surface charge of the mineral. Nevertheless, for clay minerals, the consumption and release of protons during an acid/base titration can be due to at least three processes:

- proton adsorption/desorption on the edge sites (i.e. aluminols and silanols);
- exchange reactions on basal planes to compensate the negative structural charge;
- hydrolysis of aqueous cations released during mineral dissolution.

The consumption/release of protons due to cation hydrolysis can be quantified if their total concentration is known. Hence, several samplings were performed during the titrations (for both continuous and batch methods) in order to measure the total concentration of Si, Al and Fe. Aluminum is the only element which is likely to hydrolyze in the studied pH range and which has been detected in non-negligible amounts. Measurements showed that aqueous aluminum concentrations did not vary significantly with pH and temperature. Consequently, we assumed a constant concentration of 1.6×10^{-5} mol/L (higher measured value). The aqueous aluminum speciation was then computed at each point of the titration, using the total Al concentration and the hydrolysis constants proposed by Wesolowski and Palmer (1994) at 25 and 60 °C.

Finally, the term ΔQ^{solid} is corrected for Al hydrolysis following equation

$$\Delta Q(\text{mol/g}) = (\Delta Q^{\text{solid}} - \sum_{n=0}^{4}(3-n)[\text{Al(OH)}_n^{(3-n)+}])/M \quad (3)$$

where M is the solid/solution ratio (2.5 g/L).

The contribution of Al hydrolysis to the charge balance is illustrated on Fig. 3, for an experiment performed with Na-montmorillonite at $I = 0.5$ M and 25 °C. In the modeling section, we show that ΔQ corresponds to the net proton surface excess/consumption of the solid phase.

5. Experimental results

5.1. Comparison between continuous and batch methods

Fig. 4A presents the data obtained from the continuous titration method for Na-montmorillonite at 25 °C, as a function of pH and ionic strength. Fig. 4B illustrates the results of batch experiments carried out with Na-montmorillonite at 25 °C, using two ionic strengths and two equilibration times. These diagrams show clearly that these methods do not lead to the same results. The data provided by continuous titrations show three distinct curves, with relatively smooth slopes and practically parallel. Results from the batch experiments are more scattered and vary significantly with time. Two points should be noted: first, more than 24 h are required to reach a steady state and, even after 168 h, the system is not yet equilibrated; second, this method also leads to distinct curves, depending on ionic strength, with higher slopes than those obtained with the continuous method. To interpret the strong drift in pH, we have modeled the dissolution process of montmorillonite in the conditions of our experiments and calculated the solution characteristics (e.g. speciation and pH) at equilibrium. Calculations were performed with the computer code CHESS® (Van der Lee and De Windt, 2002) along with the SUPCRT 92 database (Johnson et al., 1992). The starting conditions were as follows: 2.5 g of Na-montmorillonite in 1 L of an $HClO_4/NaClO_4$ solution at 0.5 M ionic strength and pH 4. At equilibrium, about 2.5% of the montmorillonite has dissolved leading to a pH around 5.2 and a total concentration of aqueous silica around 2×10^{-4} mol/L. Similar calculations were performed

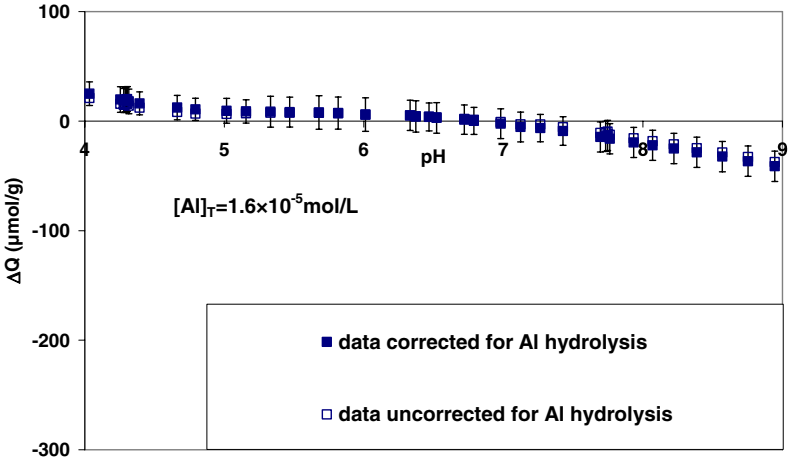

Fig. 3. Contribution of the hydrolysis of aqueous aluminum to the surface proton excess, as a function of pH (experimental conditions: 25 °C, $I = 0.5$ M, continuous titrations, Na-montmorillonite).

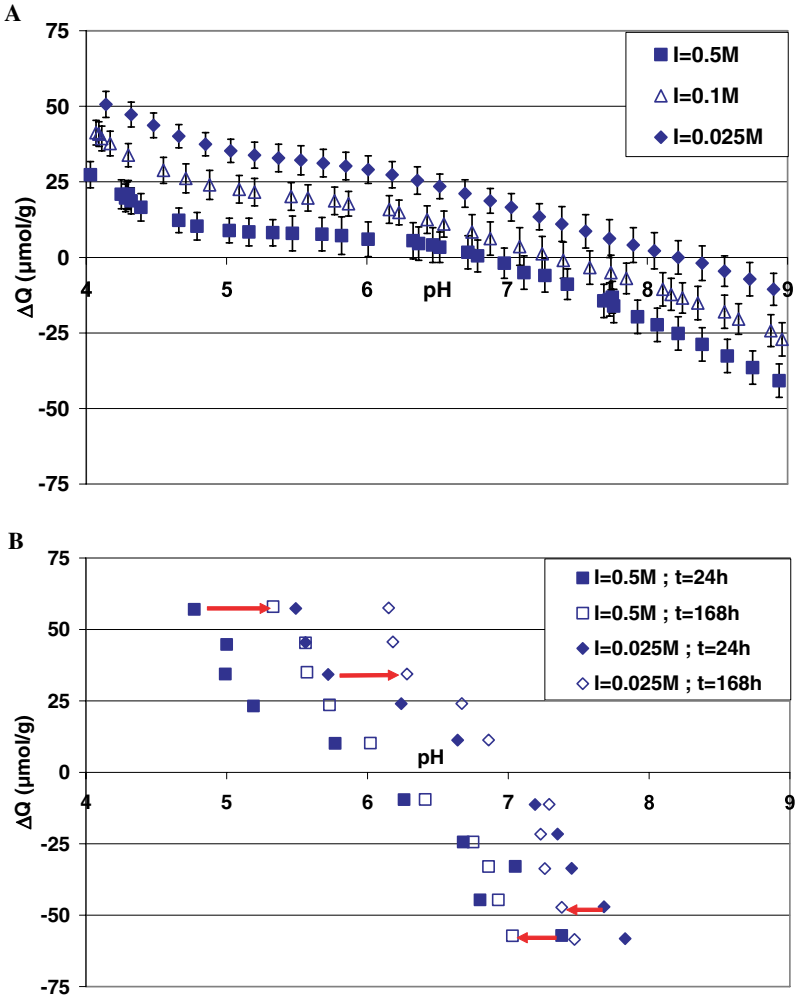

Fig. 4. Surface proton excess for Na-montmorillonite, at 25 °C, as a function of pH and ionic strength. (A) Potentiometric continuous method, (B) batch experiments for two equilibration times.

starting at alkaline pH (near 8) which leads to an equilibrium pH close to 7.5. Consequently, dissolution of the montmorillonite and hydrolysis of aqueous species can fully explain the pH drift observed during the batch experiments, whatever the initial pH conditions.

Fig. 5A and B compare the data obtained for kaolinite using both methods. The batch experiments give results very similar to those obtained with the montmorillonite. As with the continuous method, the change in pH with time can be adequately explained by geochemical equilibrium calculations taking account of the solid-phase dissolution and the hydrolysis of aqueous species. On the other hand, the continuous technique leads to a consistent data set that does not vary with ionic strength.

In view of these results, it appears that surface processes are screened during batch experiments, if not actually modified or perturbed, by reactions related to dissolution. Such a difficulty has already been evoked for more soluble minerals such as solid carbonates (Charlet et al., 1990). Consequently, the continuous method seems more suitable for studying reactions occurring at the solid surface. We therefore assume that these reactions are rapid (<10 min) and that a steady state is reached during the duration of the continuous titrations. This is in agreement with other authors, for example, Avena and De Pauli (1998), who consider that 5 min are sufficient to reach equilibrium during acid/base titrations of montmorillonite. Moreover, Bruque et al. (1980) and Bonnot-Courtois and Jaffrezic-Renault (1982) assume that short durations are sufficient to reach sorption equilibrium of lanthanides onto clays (20 min for Bruque et al.; 10 min for Bonnot-Courtois and Jaffrezic-Renault). Consequently, the continuous method is the method adopted here to determine the proton surface charge of clay minerals.

Experimental data of continuous titrations are listed for both minerals in the Appendix A, as a function of ionic strength, pH and temperature.

5.2. Ionic strength and temperature effects

The effect of the ionic strength on the net proton consumption values, calculated at 25 and 60 °C, are reported on Figs. 4A and 6A for montmorillonite and Figs. 5A and 6B for kaolinite.

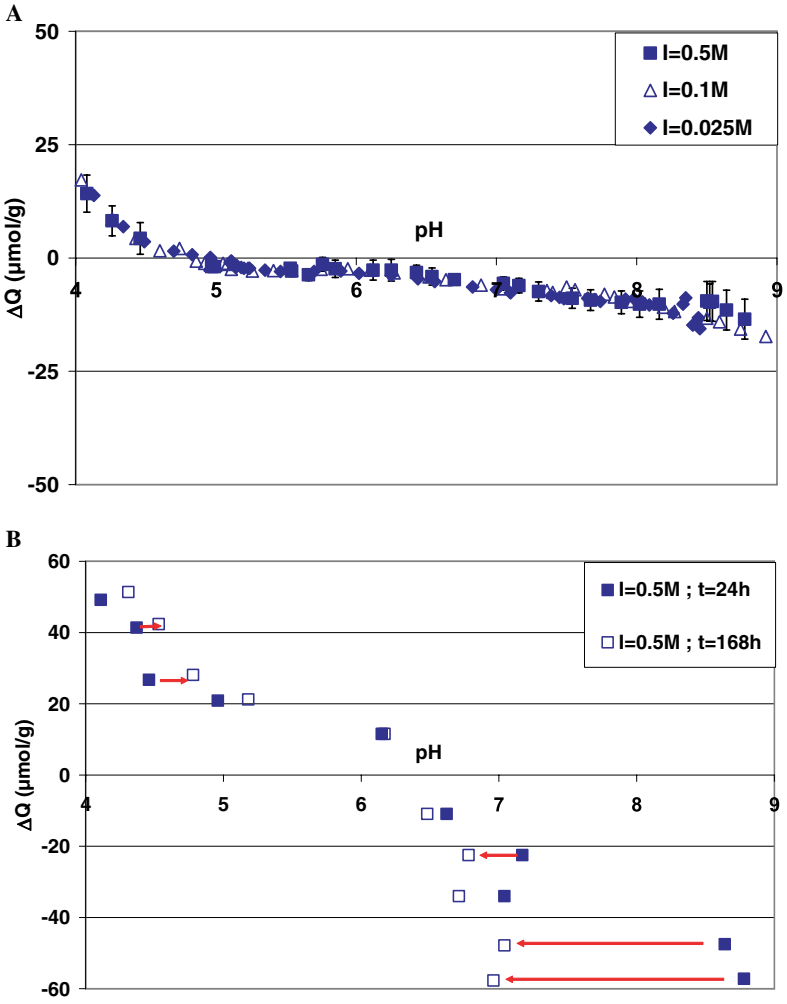

Fig. 5. Surface proton excess for kaolinite, at 25 °C, as a function of pH 7. (A) Continuous titration at three ionic strengths, (B) batch experiments for two equilibration times and $I = 0.5$ M.

The results show that the effect of ionic strength on the net proton consumption is clearly different for these two clays. Moreover, these results are also very different from those generally obtained for simple oxides, for which curves intersect at a unique point. Indeed, the kaolinite curves are superimposed, whereas the smectite curves are visibly parallel, showing an increase of the surface protonation with increasing ionic strength at a given pH. These observations are validated whatever the temperature, and are in agreement with the results of Huertas et al. (1998), Fournier (2002) and Ganor et al. (2003) for kaolinite, and Kraepiel et al. (1998), Avena and De Pauli (1998) and Tombacz et al. (2004) for montmorillonite.

Fig. 7 shows the specific effect of ionic strength on the results obtained for smectite, where the pH corresponding to zero proton surface excess is reported as a function of $\log(I)$ and compared to literature data. We note a good agreement between the different data sets. The net proton surface excess obtained at $I = 0.5$ M, at 25 and 60 °C, are compared on Fig. 8A for montmorillonite and 8B for kaolinite. The temperature increase does not appear to have a significant impact on the kaolinite net proton surface excess whereas for the montmorillonite, we observe a slight increase of the net proton consumption between pH 4 and 6, with the temperature rising from 25 to 60 °C.

6. Modeling

6.1. Models proposed in the literature

In the following discussion, we attempt to find a rational and consistent surface speciation scheme for the interpretation of experimental data as a function of both ionic strength and temperature rather than determining the most suitable complexation model (i.e. CCM, DDLM, TLM, etc.). This point is particularly important since most of the models proposed in the literature were developed to interpret data obtained at only one ionic strength, whereas no studies have so far incorporated the temperature effect. Moreover, we focus here on studies related to Na-montmorillonite, since the data obtained with this mineral appears to be more sensitive to these parameters.

Wanner et al. (1994) report continuous titrations carried out at 25 °C, between pH 4 and 10, and at $I = 0.005$, 0.05

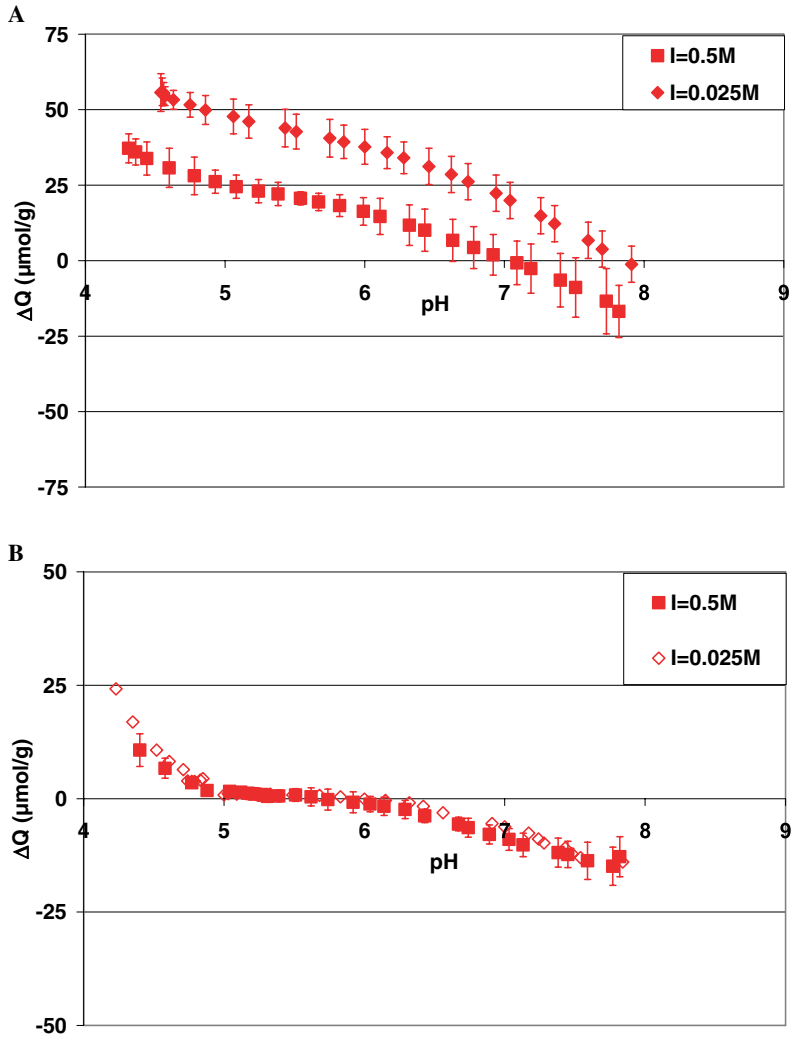

Fig. 6. Surface proton excess, at 60 °C, as a function of pH and ionic strength 8. (A) Na-montmorillonite, (B) kaolinite.

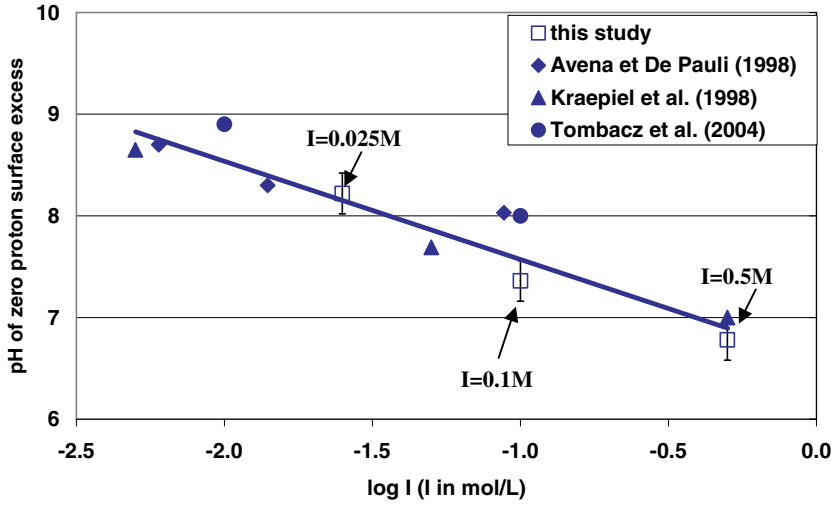

Fig. 7. Comparison with literature data of the pH values corresponding to zero proton surface excess, as a function of log(*I*), for Na-montmorillonite, at 25 °C.

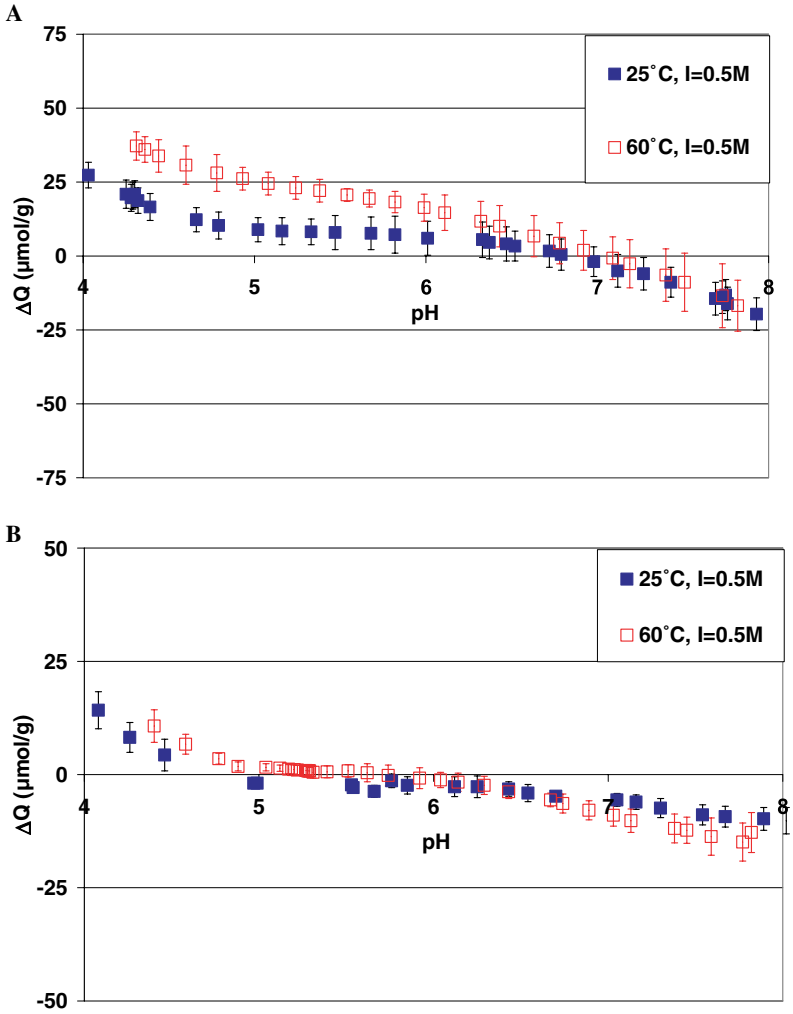

Fig. 8. Comparison between surface proton excess obtained at 25 and 60 °C in 0.5 M $NaClO_4$ solutions for: (A) montmorillonite, (B) kaolinite.

and 0.5 M ($NaNO_3$). The solid phase used by Wanner et al. (1994) exhibited a surface area of 31.53 m^2/g and a measured CEC of 108 meq/100 g. In the more acidic pH range (3.5–5), and for pH higher than 8.5, these authors obtained three distinct curves, comparable to the results presented here. In the intermediate pH range, their data are more or less superimposed. These data were modeled using the DDLM. The surface speciation scheme is very simple since it only involves one exchange site, XNa or XH, and one SOH edge site that undergoes protonation or deprotonation as a function of pH. The study of Baeyens and Bradbury (1997) involved batch experiments followed by back titrations of the supernatant, carried out at 25 °C, between pH 4 and 10 and at $I = 0.5$ and 0.1 M. These authors performed their experiments with a Na-montmorillonite exhibiting a CEC value of 87 meq/100 g and a surface area of 35 m^2/g. In this case, the results appear insensitive to the ionic strength. Bradbury and Baeyens (1997) applied a non-electrostatic model (NEM) involving three edge sites: a "strong" site, S^SOH, and two "weak" sites: $S^{w1}OH$ and $S^{w2}OH$. They did not take into account any exchange reactions. This speciation scheme implies the same pK_a values for the S^SOH and the $S^{w1}OH$ sites. Kraepiel et al. (1998) were the first authors to constrain their model to obtain a negative surface potential whatever the pH or ionic strength. Their theoretical study was based on the experimental results of Wanner et al. (1994) for montmorillonite, and those of Schindler et al. (1987) for kaolinite. They modeled this latter mineral as a non-penetrable solid phase, i.e. only surface reactions were considered. The DDLM was used along with a negative surface site X^- and one edge site, SOH. For montmorillonite, these authors developed their own surface complexation model considering a porous solid phase. In this case, the negative site X^- is located within the whole structure. Whatever the model, the pH and the ionic strength conditions, accounting for a site X^- leads to a surface potential systematically negative, in agreement with electrokinetic data (see the review of Duc et al., 2005a).

Avena and De Pauli (1998) studied the proton surface charge of a Na-montmorillonite in the range of ionic strength 0.006–0.088 M. Their mineral exhibited a surface area of 800 m^2/g and a measured CEC of 80.2 meq/100 g. The experimental data show three almost parallel curves.

These authors chose the CCM formalism and proposed a surface speciation involving a structural site X, which can be bound either to Na^+ or to H^+ to form the XNa^+ and XH^+ species, or remain uncompensated, along with an edge site SOH. Here also, the calculated surface potential is negative whatever the pH. Finally, Tombacz et al. (2004) report titration data for a Na-montmorillonite (surface area: 800 m^2/g, CEC not measured), at 25 °C and for $I = 0.01$; 0.1 and 1 M. Here again, the results lie on three distinct curves. These authors based their model on the non-penetrable solid phase of Kraepiel et al. (1998), assuming only surface sites: an exchange X^- site and an aluminol site. Nevertheless, they point out that the pK_a of this latter site is intermediate between the values for aluminol and silanol sites of simple oxides (Al_2O_3 and SiO_2). The parameters reported in these different studies are listed in Table 2.

Among the different models presented above, that of Bradbury and Baeyens (1997) cannot be adopted due to the atypical trend of their data versus ionic strength. The modeling of Wanner et al. (1994) provides two surprising results: (i) an edge site density higher than that of the structural sites and (ii) a total site density accounting for less than 5% of the total CEC. These results are hardly realistic as regards the crystallographic structure, which casts doubt on the corresponding model. The proposal by Avena and De Pauli (1998) is certainly more reasonable, but the speciation scheme involving the X, XNa^+ and XH^+ sites renders the writing of charge and mass balances very problematic. Lastly, the models proposed by Kraepiel et al. (1998) and, consequently, that of Tombacz et al. (2004), appear more realistic. The speciation scheme based on a porous solid is certainly more sophisticated, but it requires a specific surface complexation formalism and is only applicable to montmorillonite. Considering that Tombacz et al.'s (2004) model can be successfully applied to the simplest non-penetrable framework to interpret data for montmorillonite, we choose to base our modeling on this surface speciation model.

6.2. Model proposed in this study

To propose an acid/base model that can (i) reproduce the negative potential indicated by electrophoretic measurements, and (ii) take into account the crystalline structure of clays, we may consider one negative exchange site and two edge sites. The negative exchange site, X^-, can react with both H^+ and Na^+ according to the reactions:

$$X^- + H^+ = XH \quad \text{(Reaction1)}$$

$$X^- + Na^+ = XNa \quad \text{(Reaction2)}$$

Concerning the edge sites, we assume that montmorillonite and kaolinite possess silanol and aluminol sites. In agreement with literature data, we consider that aluminol sites are amphoteric (Huang, 1971; Brady, 1994; Tombacz et al., 2004) and that silanol sites can only be neutral or negative in the studied range of pH (Brady et al., 1996;

Table 2
Parameters of the acid/base models proposed in the literature for montmorillonite

Model	Site	Site density (meq/100 g)	$\log K$ $X+Na^+ = XNa^+$ (1) $X^- + Na^+ = XNa$ (2)	$\log K$ $X+H^+ = XH^+$ (1) $X^- + H^+ = XH$ (2)	$\log K$ $XNa+H^+ = XH+Na^+$	$\log K$ $\equiv SOH+H^+ = \equiv SOH_2^+$	$\log K$ $\equiv SOH = \equiv SO^- + H^+$
Bradbury and Baeyens (1997), Baeyens and Bradbury (1997) NEM	$\equiv S^sOH$	0.2	—	—	—	4.5	−7.9
	$\equiv S^{w1}OH$	4.0	—	—	—	4.5	−7.9
	$\equiv S^{w2}OH$	4.0	—	—	—	6	−10.5
Wanner et al. (1994) CCM	X	2.2	—	—	4.6	—	—
	$\equiv SOH$	2.8	—	—	—	5.4	−6.7
Kraepiel et al. (1998) DDLM	X	102	—	—	—	—	—
	$\equiv SOH$	2.8	—	—	—	5	−8.5
Avena and De Pauli (1998) CCM	X	79.6	−0.77 (1)	1.07 (1)	—	—	—
	$\equiv SOH$	4.14	—	—	—	2.97	−6.10
Tombacz et al. (2004) DDLM	X^-	100 ± 2	0.78 (2)	8.77 (2)	—	—	—
	$\equiv AlOH$	3-4	—	—	—	5.1 ± 0.1	−7.9 ± 0.1

Sverjensky and Sahai, 1998). Therefore, three reactions are taken into account:

$$\equiv AlOH + H^+ = \equiv AlOH_2^+ \quad \text{(Reaction3)}$$

$$\equiv A\mathit{lOH} = \equiv AlO^- + H^+ \quad \text{(Reaction4)}$$

$$\equiv SiOH = \equiv SiO^- + H^+ \quad \text{(Reaction5)}$$

The term ΔQ corresponds to the charge balance and can be expressed as

$$\Delta Q(\text{mol/g}) = ([M^+]^s + [\equiv AlOH_2^+] - [\equiv AlO^-] - [\equiv SiO^-] - [X^-])/M \quad (4)$$

In this equation, $[M^+]^s$ represents the quantity of compensating cations released into solution (i.e. Na^+) and M is the solid/solution ratio (2.5 g/L). According to the mass balance on the X site, this quantity is equal to

$$[M^+]^s = [X^-] + [XH] \quad (5)$$

Combining Eqs. (4) and (5), we obtain

$$\Delta Q(\text{mol/g}) = ([\equiv AlOH_2^+] - [\equiv AlO^-] - [\equiv SiO^-] + [XH])/M \quad (6)$$

Therefore, using Eq. (6), the data can be fitted as a function of pH to determine the site densities and the reactions constants. For this purpose, we used the computer code Fiteql® 3.2 (Herbelin and Westall, 1996) and the Diffuse Double Layer Model (DDLM).

6.3. Methodology

In view of the numerous parameters to be determined (5 constants and 2 site densities), and following the methodology adopted by Tombacz et al. (2004), our model is constructed in successive steps. In the first one, as a primary approximation, we consider that Na^+/H^+ exchange reactions are negligible at high ionic strength (i.e. 0.5 M). Then, we use the data obtained at $I = 0.5$ M to determine an initial set of values for the constants of reactions 3–5 as well as for the corresponding edge site densities. These parameters are then used along with the experimental data obtained at $I = 0.1$ and 0.025 M to adjust the constants for exchange reactions 1 and 2. Finally, all the parameters are adjusted again in order to achieve the best possible fit with the data obtained at 0.5 M.

To minimize the number of possible solutions, we constrain the values of some parameters. These constraints are detailed below:

- The ratio of the edge site densities, $\frac{\equiv SiOH}{\equiv AlOH}$, is in agreement with the structural formula, being fixed at a value of 2 for the montmorillonite and 1 for the kaolinite. The aluminol sites on octahedral planes of this latter mineral are not taken into account. Indeed, these sites are usually considered as unreactive due to the coordination of the oxygen ions with two Al ions (Davis and Kent, 1990).
- The total structural site density is set to the measured CEC values (87 meq/100 g for the montmorillonite and 3.7 meq/100 g for the kaolinite).
- The structural and edge sites densities are assumed to be independent of both the temperature (at least between 25 and 60 °C) and the ionic strength.

Finally, we take into account the variation of the water dissociation constant with temperature (data from Tanger and Helgeson, 1997, see Table 1).

Table 3 reports the sets of parameters allowing the best interpretation of the data obtained with montmorillonite and kaolinite at 25 and 60 °C. Fig. 9A and B compare the computed net proton surface excess for montmorillonite with the experimental points as a function of ionic strength and pH for the runs performed at 25 °C and 60 °C, respectively. Similar plots are presented on Fig. 10 A and B for kaolinite. In this case, since the calculated curves are practically superimposed, we only present the data obtained at $I = 0.5$ M. Whatever the temperature, we obtain a good agreement between calculated curves and experimental data, over the entire pH range for montmorillonite, and above pH ≈ 4.5 for kaolinite. We should emphasize here that the quality of the fit is not affected by the value of the CEC used in the model (i.e. measured or theoretical). The values of the site densities, which are expressed in mol/g, can be converted in mol/m^2 if the ''real'' surface area is known. Indeed, the specific surface area measured by the BET method is usually attributed to the sole external sur-

Table 3
Parameters of the acid/base model proposed in this study to interpret the surface proton excess of the Na-montmorillonite and kaolinite, at 25 and 60 °C

Mineral	Sites	Density (μmol g^{-1})	Surface reaction	log K (25 °C) ±0.3	log K (60 °C) ±0.3
Na-montmorillonite	≡AlOH	40.8	$\equiv AlOH + H^+ = AlOH_2^+$	5.1	6.5
			$\equiv AlOH = \equiv AlO^- + H^+$	−8.5	−8.7
	≡SiOH	81.6	$\equiv SiOH = \equiv SiO^- + H^+$	−7.9	−8.0
	X^-	871.2	$X^- + H^+ = XH$	−2.2	−2.2
			$X^- + Na^+ = XNa$	1.4	2.5
Kaolinite	≡AlOH	8.3	$\equiv AlOH + H^+ = \equiv AlOH_2^+$	4.8	5.1
			$\equiv AlOH = \equiv AlO^- + H^+$	−6.1	−6.6
	≡SiOH	8.3	$\equiv SiOH = \equiv SiO^- + H^+$	−7.7	−7.7
	X^-	37.0	$X^- + H^+ = XH$	−2.2	−2.2
			$X^- + Na^+ = XNa$	5.1	5.4

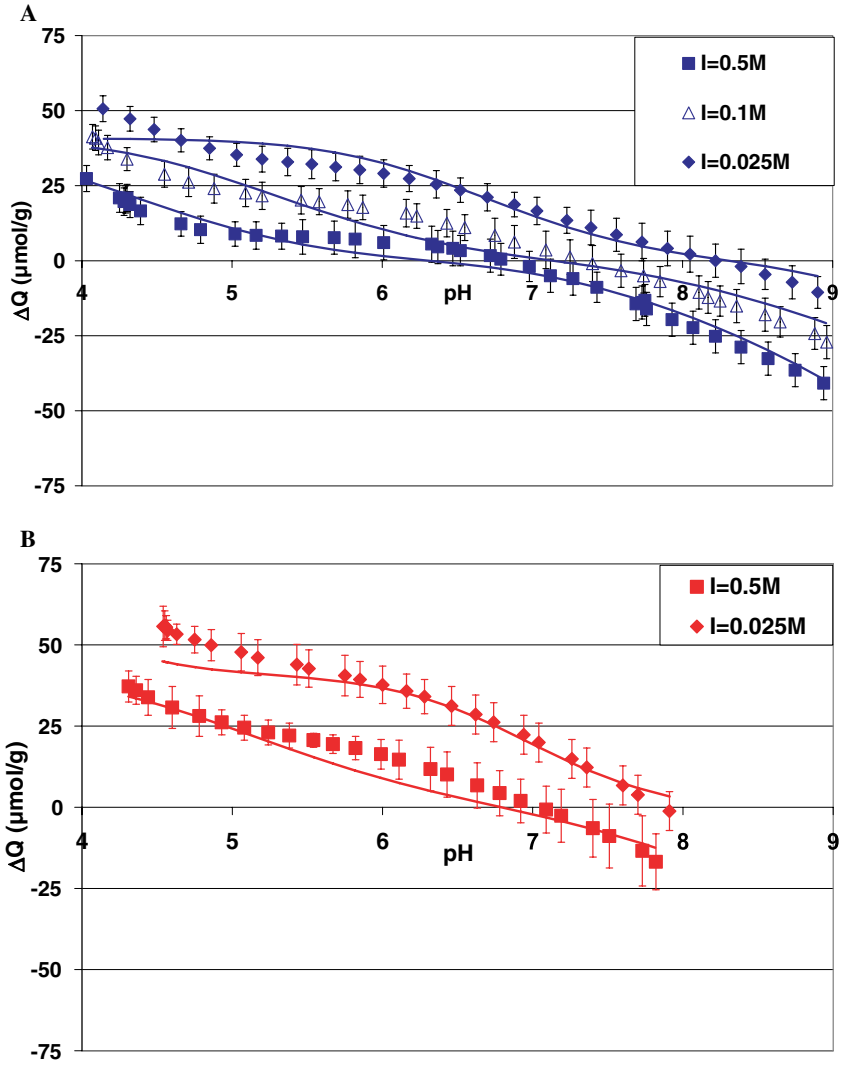

Fig. 9. Surface proton excess for the Na-montmorillonite as a function of pH and ionic strength. Comparison of values computed with the model to the experimental data (A) 25 °C, (B) 60 °C.

face. This value is certainly close to the real surface for kaolinite but, for montmorillonite, the total reactive surface is generally estimated at 700–800 m^2/g (Kraepiel et al., 1999; Tournassat et al., 2003; Tombacz et al., 2004). In consequence, we can assume that the edge sites are distributed over a restricted surface area, i.e. that measured by the B.E.T. method (24 and 10 m^2/g for the montmorillonite and the kaolinite, respectively), whereas the structural sites for montmorillonite are located on a wider surface supposed at 800 m^2/g. The data obtained in this way are reported in Table 4. The value of the structural site density for montmorillonite appears coherent with the crystal structure. As for the total edge site densities, there are in agreement with those reported in the literature, from 2 to 8 $\mu mol/m^2$ for kaolinite (Brady et al., 1996; Huertas et al., 1998), and between 2 and 5 $\mu mol/m^2$ for montmorillonite (Bradbury and Baeyens, 1997; Avena and De Pauli, 1998).

For both clays, the dissociation constants of the edge sites (i.e. ≡AlOH and ≡SiOH) obtained at 25 °C are coherent with those reported in literature for corresponding single oxides, except for the deprotonation constant of the ≡AlOH group (see for example the theoretical paper of Sverjensky and Sahai (1996) and the complete experimental review of Sahai and Sverjensky (1997)). Indeed, for corundum and alumina Sahai and Sverjensky (1997) report constants for the protonation of the ≡AlOH group from $\log K = 5.1$–6.1 whereas the value for the deprotonation constant appears to be more controversy (from −11.1 to −11.8 in Sahai and Sverjensky (1997) and from −9.8 to −10.2 in Sverjensky and Sahai (1996)). On the other hand, for quartz, the deprotonation constant of the ≡SiOH group is estimated to $\log K = -7.7 \pm 0.1$ (Sverjensky and Sahai, 1996; Sahai and Sverjensky, 1997).

The data proposed for reactions 1 and 2 allow to compute the constant for the Na/H exchange reaction ($XNa + H^+ = XH + Na^+$) at 25 °C: $\log K_{Na/H} = -3.6$ for Na-montmorillonite and −7.2 for kaolinite. An overview

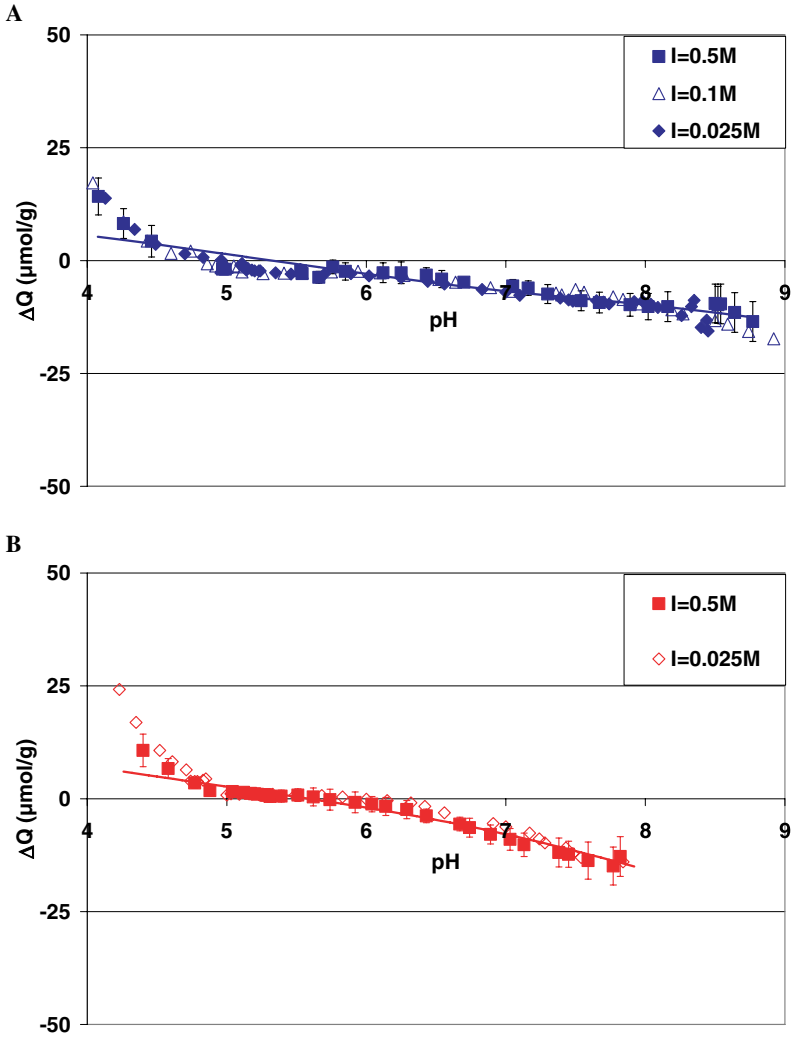

Fig. 10. Surface proton excess for the kaolinite as a function of pH and ionic strength. Comparison of values computed with the model to the experimental data (A) 25 °C, (B) 60 °C.

Table 4
Basal and edge sites densities expressed by unit surface for montmorillonite and kaolinite (see text)

Mineral	Sites	Density (μmol m^{-2})
Na-montmorillonite	≡AlOH	1.70 [a]
$S_{BET} = 24\ m^2\ g^{-1}$	≡SiOH	3.40 [a]
$S_{Tot} = 800\ m^2\ g^{-1}$	X^-	1.09 [b]
Kaolinite	≡AlOH	0.83
$S_{BET} = 10\ m^2\ g^{-1}$	≡SiOH	0.83
	X^-	3.70

[a] Calculated from the surface area measured by the B.E.T. method.
[b] Calculated with a total reactive surface of 800 $m^2\ g^{-1}$.

of the literature data results in a wide range of values suggested for this constant. For example, Charlet and Tournassat (2005) and Tournassat et al. (2004b), use a value $\log K_{Na/H} = 0$ to fit their data, the model from Tombacz and Szekeres (2004) results in a value of 7.99, Janek and Lagaly (2001) propose a measured value at −2.8 and Fletcher and Sposito (1989) report an average value of 0.1 from a review of the previous literature data. In view of these discrepancies, and considering the lack of studies specifically focused on the measurement of this constant, it is difficult, at present, to discuss the reliability of the values we propose.

It can be seen from Table 3 that temperature has a generally weak influence on the values of the reaction constants. A change of nearly one log unit is found only in the case of the protonation constant for the aluminol site on montmorillonite. This leads to neutral edges at pH 6.5 ± 0.3 at 25 °C and 6.8 ± 0.3 at 60 °C for this mineral. The corresponding value for kaolinite is at pH 5.4 ± 0.3 irrespective of the temperature.

Contributions of the X^- and XNa species to the total structural site density of montmorillonite are reported, at 25 °C, as a function of pH and ionic strength on Fig. 11A and B, respectively. A general view of the importance of all the surface species is given on Fig. 12, at $I = 0.5$ M. The fraction of the uncompensated X^- species is greater under acidic conditions and at low ionic strength,

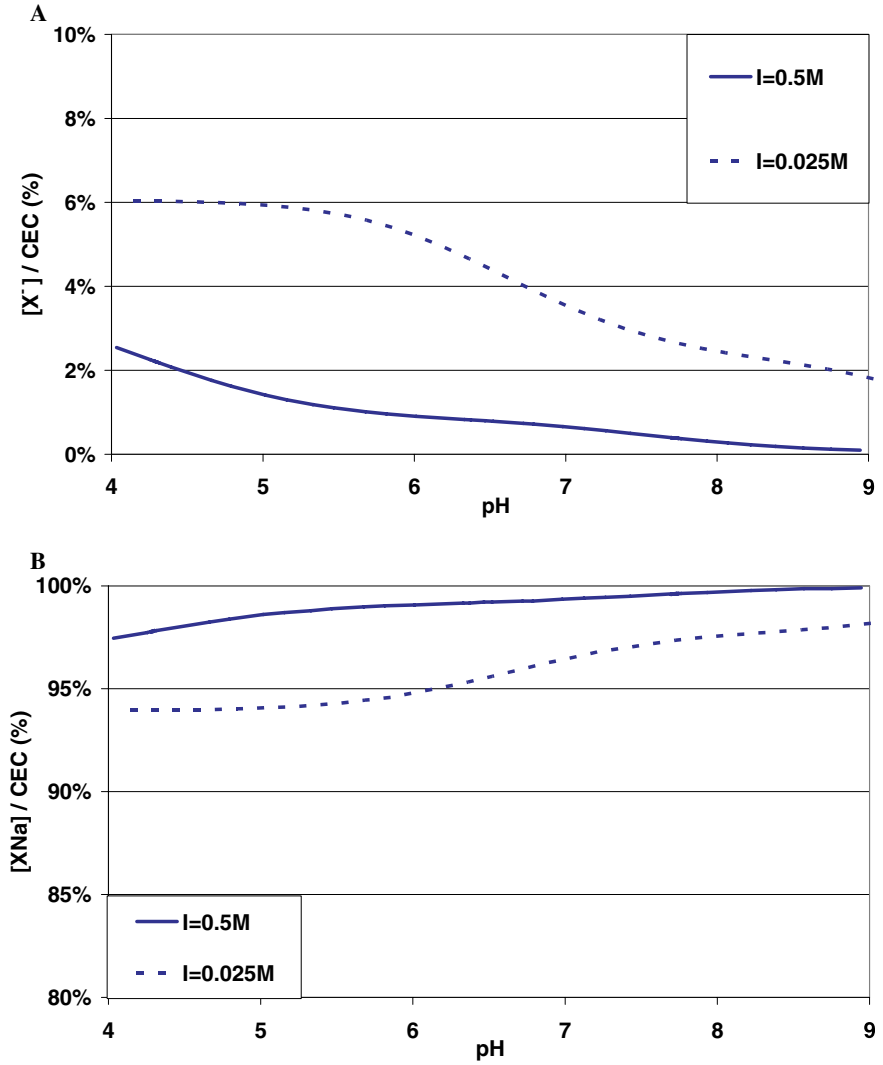

Fig. 11. Fractions of X^- (A) and XNa (B) relative to the CEC, calculated as a function of pH and ionic strength, for the Na-montmorillonite, at 25 °C.

but is always very small (<6%). This is in agreement with the conclusions of Avena and De Pauli (1998); Kraepiel et al. (1998); Tombacz et al. (2004); Duc et al. (2005a). On the other hand, the proportion of the XNa species is always predominant, accounting for 95% or more of the total structural site density.

7. Concluding remarks

The first aim of this study was to compare two experimental protocols to measure the acid/base surface properties of montmorillonite and kaolinite. Tests carried out with the same materials and experimental conditions show that continuous titration and batch methods provide notably different results. Continuous titration leads to a smooth and consistent data set, whereas batch experiments involve a drastic pH drift over long time period. This behavior can be clearly related to a significant dissolution of the mineral and the associated hydrolysis of aqueous species. Over a long time scale, these reactions are assumed to overlap with surface processes and/or modify the state and speciation of the mineral surface. On the other hand, our results show that, whatever the method used, the curves representing the proton surface excess as a function of ionic strength are almost parallel for montmorillonite and superimposed for kaolinite. We conclude that the different results reported in the literature (for example, Baeyens and Bradbury, 1997) cannot be attributed to the experimental protocol but rather to the solid purification method (cf. Duc et al., 2005b for discussion).

The second aim was to provide a consistent data set as a function of both ionic strength and temperature for two contrasted clay minerals. The data acquired for montmorillonite and kaolinite as a function of ionic strength are significantly different. This difference is correlated with the negative structural charge characterizing these minerals. On the other hand, temperature appears to have only a weak influence on the surface protonation of both minerals.

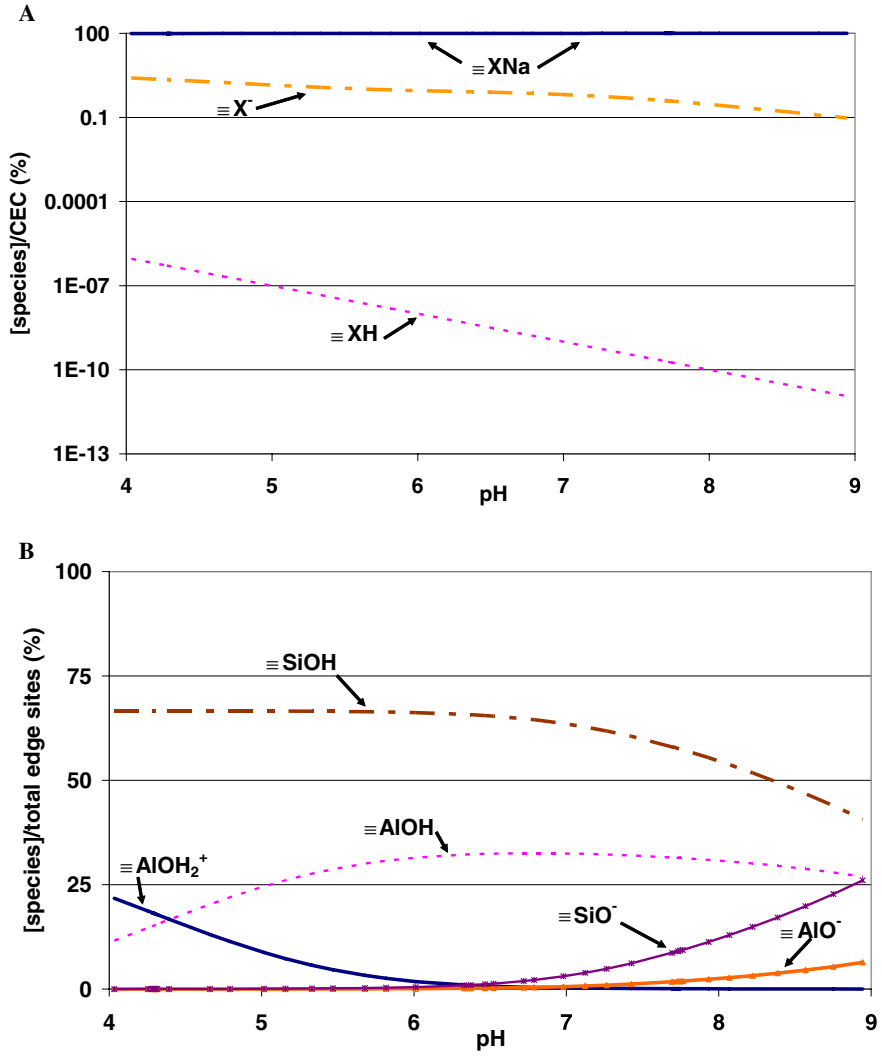

Fig. 12. Speciation of exchange (A) and edge (B) sites as a function of pH, for the Na-montmorillonite, at 25 °C and 0.5 M $NaClO_4$ solution.

Finally, we critically analyze various models accounting for the dependence of the proton surface excess of clays on ionic strength. This review clearly demonstrates that a fraction of the structural negative charge of the mineral must remain uncompensated to fit correctly with the experimental data. Accordingly, the surface speciation scheme proposed here involves an exchange site that is able to react with Na^+ or H^+ ions or remain uncompensated, along with two edge sites assumed to correspond to aluminol and silanol sites. This modeling approach, as others previously proposed in the literature, implies a very small fraction of uncompensated structural sites X^- (<6% of the total CEC), especially in the acidic pH range. Although this result is not yet fully understood, it is probably related to kinetic processes or special interactions between particles.

In conclusion, we note that the model parameters discussed here are closely dependent on one decisive variable, namely, the solid-phase specific area. Indeed, the value of the "true" specific area (between about 30 and 800 m^2/g) is crucial because it directly controls the surface site density. Much further work is also needed to propose reliable values for the Na/H exchange reaction constants in order to better constrain models dedicated to the surface chemistry of clays.

Acknowledgments

This research was supported by grants from ANDRA (Agence Nationale pour la gestion des Déchets Radioactifs) and EDF (Electricité De France). The authors thank Pat Brady and two anonymous reviewers for their substantial contribution to improve the paper. A big thank you to Pascale Benezeth for her patience and help with reading the text.

Associate editor Johnson R. Haas

Appendix A. Surface proton excess (ΔQ) of the Na-montmorillonite and the kaolinite as a function of pH, ionic strength and temperature, obtained by the continuous method

Surface proton excess for Na-montmorillonite as a function of pH and ionic strength, at 25 °C

$I = 0.5$ M			$I = 0.1$ M			$I = 0.025$ M		
pH	ΔQ (10^6 mol/g)	Error on ΔQ (10^6 mol/g)	pH	ΔQ (10^6 mol/g)	Error on ΔQ (10^6 mol/g)	pH	ΔQ (10^6 mol/g)	Error on ΔQ (10^6 mol/g)
4.03	27.36	4.32	4.07	41.28	4.08	4.14	50.64	4.32
4.25	20.88	4.8	4.09	40.8	4.08	4.32	47.28	4.08
4.3	20.88	4.56	4.11	39.36	4.08	4.48	43.68	4.08
4.29	20.4	4.56	4.17	37.68	4.08	4.66	40.08	3.84
4.28	19.68	4.56	4.3	33.84	3.84	4.85	37.44	3.84
4.32	18.72	4.32	4.55	28.8	4.32	5.03	35.28	3.84
4.39	16.56	4.56	4.71	26.16	4.8	5.2	33.84	4.32
4.66	12.24	4.08	4.88	24	4.8	5.37	32.88	4.56
4.79	10.32	4.56	5.09	22.56	4.56	5.53	32.16	4.8
5.02	8.88	4.08	5.2	21.6	4.56	5.69	31.2	4.56
5.16	8.4	4.56	5.46	20.16	4.56	5.85	30.24	4.56
5.33	8.16	4.32	5.58	19.68	4.32	6.01	29.04	4.56
5.47	7.92	5.76	5.77	18.72	4.56	6.18	27.36	4.32
5.68	7.68	5.52	5.87	17.76	4.08	6.36	25.44	4.56
5.82	7.2	6.24	6.16	15.84	4.56	6.52	23.52	4.08
6.01	6	5.76	6.23	14.88	4.08	6.7	21.12	4.56
6.33	5.52	6	6.43	12.48	4.56	6.88	18.72	4.08
6.37	4.56	5.52	6.55	11.04	4.32	7.03	16.56	4.56
6.47	4.08	5.76	6.75	8.4	5.76	7.23	13.44	4.32
6.52	3.36	5.04	6.88	6.24	5.52	7.39	11.04	5.76
6.72	1.68	5.52	7.09	3.6	6.24	7.56	8.64	5.52
6.79	0.48	5.28	7.25	1.2	5.76	7.73	6.24	6.24
6.98	−1.92	5.04	7.4	−0.96	6	7.9	4.08	5.76
7.12	−5.04	5.52	7.59	−3.36	5.52	8.05	2.16	6
7.27	−6	5.52	7.74	−5.04	5.76	8.22	0	5.52
7.43	−8.88	5.04	7.85	−6.96	5.04	8.39	−1.92	5.76
7.75	−13.2	5.28	8.11	−10.56	5.52	8.55	−4.56	5.04
7.73	−13.92	5.52	8.17	−12.24	5.28	8.73	−7.2	5.52
7.69	−14.4	5.52	8.25	−13.44	5.04	8.9	−10.56	5.28
7.76	−16.08	5.52	8.36	−15.12	5.52			
7.93	−19.68	5.52	8.55	−18	5.52			
8.07	−22.32	5.52	8.65	−20.4	5.04			
8.22	−25.2	5.52	8.88	−24.24	5.28			
8.39	−28.8	5.52	8.96	−27.12	5.52			
8.57	−32.64	5.52						
8.75	−36.48	5.52						
8.94	−40.8	5.52						

Surface proton excess for kaolinite as a function of pH and ionic strength, at 25 °C

$I = 0.5$ M			$I = 0.1$ M			$I = 0.025$ M		
pH	ΔQ (10^6 mol/g)	Error on ΔQ (10^6 mol/g)	pH	ΔQ (10^6 mol/g)	Error on ΔQ (10^6 mol/g)	pH	ΔQ (10^6 mol/g)	Error on ΔQ (10^6 mol/g)
4.08	14.2	4.1	4.04	17.2	5.4	4.13	13.8	5
4.26	8.2	3.3	4.26	8.6	4.2	4.34	6.9	4.7
4.46	4.3	3.5	4.43	4.3	3.1	4.49	3.6	4
4.97	−1.9	1	4.6	1.6	3.7	4.7	1.5	2.8
4.99	−1.9	1	4.74	2.1	2.7	4.83	0.7	1.4
5.53	−2.3	1.1	4.86	−0.7	1.1	4.96	0.1	1.4
5.54	−2.9	1.2	4.92	−1.2	1.2	5.1	−1	1.3
5.66	−3.7	1.3	4.96	−1.4	1.2	5.15	−1.7	1.3
5.76	−1.4	1.5	4.96	−1.6	1.2	5.18	−2.1	1.3
5.85	−2.4	1.9	4.99	−1.6	1.4	5.2	−2.3	1.2
6.12	−2.7	2.2	5	−1.5	1.8	5.23	−2.3	1.2
6.25	−2.7	2.4	5.05	−1.2	2.3	5.24	−2.3	1.4
6.43	−3.2	1.6	5.08	−1.4	2.5	5.11	−0.7	1.7

(*continued on next page*)

Appendix A (*continued*)

$I = 0.5$ M			$I = 0.1$ M			$I = 0.025$ M		
pH	ΔQ (10^6 mol/g)	Error on ΔQ (10^6 mol/g)	pH	ΔQ (10^6 mol/g)	Error on ΔQ (10^6 mol/g)	pH	ΔQ (10^6 mol/g)	Error on ΔQ (10^6 mol/g)
6.54	−4.1	1.9	5.11	−2.5	1.6	5.11	−0.7	1.9
6.7	−4.8	1.1	5.26	−2.9	1.7	5.11	−1.2	1.3
7.05	−5.6	1.4	5.41	−2.8	1.3	5.14	−2.1	1.2
7.16	−6.1	1.6	5.54	−2.7	1.3	5.35	−2.7	1.7
7.3	−7.4	2.1	5.75	−2.5	1.5	5.46	−3	2
7.54	−8.9	2.2	5.94	−2.4	2.1	5.7	−3	2
7.67	−9.3	2.3	6.1	−2.7	2.3	5.89	−2.9	2.2
7.89	−9.8	2.5	6.27	−3.3	2.4	6.02	−3.4	2.1
8.02	−10.2	2.9	6.52	−4.2	2.4	6.25	−3.8	2.9
8.16	−10.2	3.3	6.64	−4.8	2.7	6.44	−4.6	3.4
8.52	−9.8	4.1	6.89	−6	3.4	6.56	−5.2	4.1
8.5	−9.5	4.3	7.04	−6.8	4.2	6.83	−6.4	4.2
8.54	−9.6	4.4	7.36	−7.2	4.3	7	−7	4.2
8.64	−11.5	4.4	7.4	−7.6	4.4	7.1	−7.7	4.6
8.77	−13.5	4.4	7.5	−6.4	4.5	7.39	−8.3	4.4
			7.56	−7	4.4	7.45	−8.7	4.7
			7.77	−8	4.5	7.48	−9	4.7
			7.84	−8.6	4.6	7.65	−8.9	4.8
			7.97	−9.6	4.6	7.7	−9.2	4.9
			8.19	−10.9	4.6	7.74	−9.6	4.7
			8.27	−11.8	4.7	7.92	−9.1	5
			8.5	−13.3	4.8	7.98	−9	5
			8.59	−14.1	4.9	8.04	−9.7	5.1
			8.74	−15.7	4.9	8.09	−10.4	5.2
			8.92	−17.3	5	8.35	−8.8	5.2
						8.33	−10.2	5.2
						8.26	−12.2	5.3
						8.44	−13.2	5.3
						8.4	−14.8	5.3
						8.45	−15.6	5.3

Surface proton excess for Na-montmorillonite as a function of pH and ionic strength, at 60 °C

$I = 0.5$ M			$I = 0.025$ M		
pH	ΔQ (10^6 mol/g)	Error on ΔQ (10^6 mol/g)	pH	ΔQ (10^6 mol/g)	Error on ΔQ (10^6 mol/g)
4.31	37.2	4.8	4.54	55.68	6.24
4.36	36	4.32	4.55	55.92	4.56
4.44	33.84	5.52	4.56	55.44	3.6
4.6	30.72	6.48	4.57	54.48	3.12
4.78	28.08	6.24	4.63	53.28	3.12
4.93	26.16	3.84	4.75	51.6	4.08
5.08	24.48	3.84	4.86	49.92	4.8
5.24	23.04	3.84	5.06	47.76	5.76
5.38	22.08	3.84	5.17	46.08	5.52
5.54	20.64	2.16	5.43	43.92	6.24
5.67	19.44	2.88	5.51	42.72	5.76
5.82	18.24	3.6	5.75	40.56	6.24
5.99	16.32	4.56	5.85	39.36	5.52
6.11	14.64	6	6	37.68	5.76
6.32	11.76	6.72	6.16	35.76	5.28
6.43	10.08	6.96	6.28	34.08	5.28
6.63	6.72	6.96	6.46	31.2	6
6.78	4.32	6.96	6.62	28.56	6
6.92	1.92	6.72	6.74	26.16	6
7.09	−0.72	7.2	6.94	22.32	6
7.19	−2.64	8.16	7.04	19.92	6
7.4	−6.48	8.88	7.26	14.88	6

Appendix A (*continued*)

$I = 0.5$ M			$I = 0.025$ M		
pH	ΔQ (10^6 mol/g)	Error on ΔQ (10^6 mol/g)	pH	ΔQ (10^6 mol/g)	Error on ΔQ (10^6 mol/g)
7.51	−8.88	9.84	7.36	12.24	6
7.73	−13.44	10.8	7.6	6.72	6
7.82	−16.8	8.64	7.7	3.84	6
			7.91	−1.2	6

Surface proton excess for kaolinite as a function of pH and ionic strength, at 60 °C

$I = 0.5$ M			$I = 0.025$ M		
pH	ΔQ (10^6 mol/g)	Error on ΔQ (10^6 mol/g)	pH	ΔQ (10^6 mol/g)	Error on ΔQ (10^6 mol/g)
4.40	10.7	3.6	4.23	24.2	6.6
4.58	6.7	2.2	4.35	16.9	4
4.77	3.5	1.2	4.52	10.7	4
4.88	1.8	1	4.61	8.2	3.6
5.04	1.6	0.8	4.71	6.4	3.2
5.12	1.4	0.7	4.74	3.9	2.1
5.17	1.2	1	4.77	3.8	2
5.20	1.1	1	4.79	3.8	2
5.22	1	1	4.83	4.1	2
5.27	0.9	1	4.85	4.4	1.9
5.28	0.8	1	5.00	0.8	0.8
5.29	0.8	0.8	5.03	1.1	0.8
5.28	0.8	1	5.09	1	0.6
5.31	0.5	1.3	5.18	1.1	0.6
5.39	0.6	1.3	5.33	1	0.8
5.51	0.8	1.4	5.49	0.8	0.8
5.62	0.4	2	5.68	0.7	0.8
5.74	−0.2	2.3	5.83	0.4	0.9
5.92	−0.8	2.3	6.00	−0.1	1.1
6.04	−1.2	1.7	6.15	−0.4	1.3
6.14	−1.7	2	6.32	−0.9	1.4
6.29	−2.4	2	6.42	−1.7	1.4
6.43	−3.8	1.5	6.56	−3.1	2.1
6.67	−5.6	1.5	6.91	−5.5	2.3
6.74	−6.4	2.1	7.00	−6.2	2.1
6.89	−7.9	2.1	7.17	−7.6	2.1
7.03	−9	2.4	7.24	−8.9	2.3
7.13	−10.2	2.6	7.28	−9.8	2.6
7.45	−12.3	2.9	7.43	−10.9	2.9
7.38	−11.9	3.2	7.48	−12.2	3.2
7.59	−13.7	4.1	7.54	−13	4
7.77	−14.9	4.2	7.84	−14	4.2
7.82	−12.8	4.4			

References

Abendroth, R.P., 1970. Behavior of pyrogenic silica in simple electrolytes. *J. Colloid Interface Sci.* **34**, 591–596.

Angove, M.J., Johnson, B.B., Wells, J.D., 1998. The influence of temperature on the adsorption of cadmium (II) and cobalt (II) on kaolinite. *J. Colloid Interface Sci.* **204**, 93–103.

Avena, M.J., De Pauli, C.P., 1998. Proton adsorption and electrokinetics of an Argentinean montmorillonite. *J. Colloid Interface Sci.* **202**, 195–204.

Baeyens, B., Bradbury, M.H., 1997. A mechanistic description of Ni and Zn sorption on Na-montmorillonite. Part I: titration and sorption measurements. *J. Contam. Hydrol.* **27**, 199–222.

Bauer, A., 1997. Etude du comportement des smectites et de la kaolinite dans des solutions potassiques (0,1–4M). Ph. D. Thesis, Université Pierre et Marie Curie (Paris VI), France, 310p.

Bérubé, Y.G., Debruyn, P.L., 1968. Adsorption at the rutile-solution interface. I. Thermodynamic and experimental study. *J. Colloid Interface Sci.* **27**, 305–318.

Blesa, M.A., Figliolia, N.M., Maroto, A.J.G., Regazzoni, A.E., 1984. The influence of temperature on the interface magnetite—aqueous electrolyte solution. *J. Colloid Interface Sci.* **101**, 410–418.

Bonnot-Courtois, C., Jaffrezic-Renault, N., 1982. Etude des échanges entre terres rares et cations interfoliaires de deux argiles. *Clay Miner.* **17**, 409–420.

Bouchet, A., Meunier, A., Sardini, P., 2000. Minéraux argileux: structure cristalline, identification par diffraction des rayons X. Bull. Centre Rech. Elf Explor. Prod., Mém. 23, 136 p.

Bradbury, M.H., Baeyens, B., 1997. A mechanistic description of Ni and Zn sorption on Na-montmorillonite. Part II: modeling. *J. Contam. Hydrol.* **27**, 223–248.

Brady, P.V., 1992. Silica surface chemistry at elevated temperatures. *Geochim. Cosmochim. Acta* **56**, 2941–2946.

Brady, P.V., 1994. Alumina surface chemistry at 25, 40, and 60 °C. *Geochim. Cosmochim. Acta* **58**, 1213–1217.

Brady, P.V., Walther, J.V., 1992. Surface chemistry and silicate dissolution at elevated temperatures. *Am. J. Sci.* **292**, 639–658.

Brady, P.V., Cygan, R.T., Nagy, K.L., 1996. Molecular controls on kaolinite surface charge. *J. Colloid Interface Sci.* **183**, 356–364.

Bruque, S., Mozas, T., Rodriguez, A., 1980. Factors influencing the retention of lanthanides ions by montmorillonite. *Clay Miner.* **15**, 413–420.

Buck, R.P., Rondinini, S., Covington, A.K., Baucke, F.G.K., Brett, C.M.A., Camoes, M.F., Milton, M.J.T., Mussini, T., Naumann, R., Pratt, K.W., Spitzer, P., Wilson, G.S., 2002. Measurement of pH. Definition, standards, and procedures (IUPAC Recommendations 2002). *Pure Appl. Chem.* **74**, 2169–2200.

Charlet, L., Wersin, p., Stumm, W., 1990. Surface charge of $MnCO_3$ and $FeCO_3$. *Geochim. Cosmochim. Acta* **54**, 2329–2336.

Charlet, L., Tournassat, C., 2005. Fe(II)–Na(I)–Ca(II) cation exchange on montmorillonite in chloride medium: evidence for preferential clay adsorption of ions pairs in marine environment. *Aquat. Geochem.* **11**, 115–137.

Coppin, F., Berger, G., Bauer, A., Castet, S., Loubet, M., 2002. Sorption of lanthanides on smectite and kaolinite. *Chem. Geol.* **182**, 57–68.

Davis, J.A., Kent, D.B., 1990. Surface complexation modeling in aqueous geochemistry: mineral-water interface geochemistry. *Rev. Miner.* **23**, 177–260.

Du, Q., Sun, Z., Forsling, W., Tang, H., 1997. Acid-base properties of aqueous illite surfaces. *J. Colloid Interface Sci.* **187**, 221–231.

Duc, M., Gaboriaud, F., Thomas, F., 2005a. Sensitivity of the acid-base properties of clays to the methods of preparation and measurement. 1—Literature review. *J. Colloid Interface Sci.* **289**, 139–147.

Duc, M., Gaboriaud, F., Thomas, F., 2005b. Sensitivity of the acid-base properties of clays to the methods of preparation and measurement. 2—Evidence from continuous potentiometric titrations. *J. Colloid Interface Sci.* **289**, 148–156.

Fletcher, P., Sposito, G., 1989. The chemical modeling of clay/electrolyte interactions for montmorillonite. *Clay Miner.* **24**, 375–391.

Fournier, P., 2002. Influence des acides organiques et des argiles sur la mobilité du plomb et du strontium dans les milieux naturels. Ph. D. Thesis, Université Paul Sabatier, Toulouse, France, 207p.

Ganor, J., Cama, J., Metz, V., 2003. Surface protonation data of kaolinite. Reevaluation based on dissolution experiments. *J. Colloid Interface Sci.* **264**, 67–75.

Herbelin, A.L., Westall, J.C., 1996. FITEQL version 3.2, a computer program for determination of chemical equilibrium constants from experimental data. Department of Chemistry, Oregon State University, Corvallis.

Hu, Y., Liu, X., 2003. Chemical composition and surface property of kaolins. *Miner. Eng.* **16**, 1279–1284.

Huang, C.P., 1971. The chemistry of the alminium oxide-electrolyte interface. Ph.D. Thesis, Harvard University.

Huang, C.P., Stumm, W., 1973. Specific adsorption of cations on hydrous γ-Al_2O_3. *J. Colloid Interface Sci.* **43**, 409–420.

Huertas, F.J., Chou, L., Wollast, R., 1998. Mechanism of kaolinite dissolution at room temperature and pressure: part 1. Surface speciation. *Geochim. Cosmochim. Acta* **62**, 417–431.

Hussain, S.A., Demirci, S., Ozbayoglu, G., 1996. Zeta potential measurements on three clays from turkey and effects of clays on coal flotation. *J. Colloid Interface Sci.* **184**, 535–541.

Janek, M., Lagaly, G., 2001. Proton saturation and rheological properties of smectite dispersions. *Appl. Clay Sci.* **19**, 121–130.

Johnson, J.W., Oelkers, E.H., Helgeson, H.C., 1992. SUPCRT92: a software package for calculating the standard molars thermodynamic properties of minerals, gases, aqueous species and reactions from 1 to 5000 bars and 0 to 1000 °C. *Comput. Geosci.* **18**, 899–947.

Kita, H., Henmi, N., Shimazu, K., Hattori, H., Tanabe, K., 1981. Measurement of acid-base properties on metal oxide surfaces in aqueous solutions. *J. Chem. Soc. Faraday Trans.* **77**, 2451–2463.

Kraepiel, A.M., Keller, K., Morel, F.M.M., 1998. On the acid-base chemistry of permanently charged minerals. *Environ. Sci. Technol.* **32**, 2829–2838.

Kraepiel, A.M., Keller, K., Morel, F.M.M., 1999. A model for metal adsorption on montmorillonite. *J. Colloid Interface Sci.* **210**, 43–54.

Machesky, M., Wesolowxki, D.J., Palmer, D.A., Ridley, M.K., 2001. On the temperature dependence of intrinsic surface protonation equilibrium constants: an extension of the revised MUSIC model. *J. Colloid Interface Sci.* **239**, 314–327.

Meier, L.P., Kahr, G., 1999. Determination of the cation exchange capacity (CEC) of clay minerals using the complexes of copper (II) ion with triethylenetetramine and tetraethylenepentamine. *Clay. Clay Miner.* **47**, 386–388.

Missana, T., Adell, A., 2000. On the applicability of DLVO theory to the prediction of clay colloids stability. *J. Colloid Interface Sci.* **230**, 150–156.

Mustapha, S., Dilara, B., Neelofer, Z., Naeem, A., Tasleem, S., 1998. Temperature effect on the surface charge properties of γ-Al_2O_3. *J. Colloid Interface Sci.* **204**, 284–293.

Sahai, N., Sverjensky, D.A., 1997. Evaluation of internally consistent parameters for the triple-layer model by the systematic analysis of oxide surface titration data. *Geochim. Cosmochim. Acta* **61**, 2801–2826.

Sauzeat, E., Guillaume, D., Neaman, A., Peiffert, C., Ruck, R., Dubessy, J., Cathelineau, M., Villieras, F., Yvon, J., 2002. Caractérisation minéralogique, cristallochimique et texturale de l'argile MX-80. Rapport ANDRA C. RP. 0LEM 01-001.

Schindler, P.W., Liechti, P., Westall, J.C., 1987. Adsorption of copper, cadmium and lead from aqueous solution to the kaolinite/water interface. *Neth. J. Agr. Sci.* **35**, 219–230.

Schroth, B.K., Sposito, G., 1997. Surface charge properties of kaolinite. *Clay. Clay Miner.* **45**, 85–91.

Shen, J., Ebner, A.D., Ritter, J.A., 1999. Points of zero charge and intrinsic equilibrium constants of silica–magnetite composite oxides. *J. Colloid Interface Sci.* **214**, 333–343.

Schulthess, C.P., Sparks, D.L., 1986. Back titration technique for proton isotherm modeling of oxide surfaces. *Soil. Sci. Soc. Am. J.* **50**, 1406–1411.

Sinitsyn, V.A., Aja, S.U., Kulik, D.A., Wood, S.A., 2000. Acid-base surface chemistry and sorption of some lanthanides on K^+-saturated marblehead illite: I. Results of an experimental investigation. *Geochim. Cosmochim. Acta* **64**, 182–194.

Sondi, I., Stubicar, M., Pravdic, V., 1997. Surface properties of ripidolite and beidellite clays modified by high-energy ball mining. *Colloid. Surf. A Physicochem. Eng. Aspects* **127**, 141–149.

Sverjensky, G., Sahai, N., 1996. Theoretical prediction of single-site surface-protonation equilibrium constants for oxides and silicates in water. *Geochim. Cosmochim. Acta* **60**, 3773–3797.

Sverjensky, D.A., Sahai, N., 1998. Theoretical prediction of single-site enthalpies of surface protonation for oxides and silicates in water. *Geochim. Cosmochim. Acta* **62**, 3703–3716.

Tanger, J.C., Helgeson, H.C., 1997. Revised equation of state for the standard partial molal properties of ions and electrolytes. *Am. J. Sci.* **288**, 19–98.

Tertre, E., Berger, G., Castet, S., Loubet, M., Giffaut, E., 2005. Experimental sorption of Ni^{2+}, Cs^+ and Ln^{3+} onto a montmorillonite up to 150 °C. *Geochim. Cosmochim. Acta* **69**, 4937–4948.

Thomas, F., Michot, L.J., Vantelon, D., Montarges, E., Prélot, B., Cruchaudet, M., Delon, J.F., 1999. Layer charge and electrophoretic molibity of smectites. *Colloid. Surf. A Physicochem. Eng. Aspects* **159**, 351–358.

Tombacz, E., Nyilas, T., Libor, Z., Csanaki, C., 2004. Surface charge heterogeneity and aggregation of clay lamellae in aqueous suspensions. *Progr. Colloid. Polym. Sci.* **125**, 206–215.

Tombacz, E., Szekeres, M., 2004. Colloidal behavior of aqueous montmorillonite suspensions: the specific role of pH in the presence of indifferent electrolytes. *Appl. Clay Sci.* **27**, 75–94.

Tournassat, C., Neaman, A., Villiéras, F., Bosbach, D., Charlet, L., 2003. Nanomorphology of montmorillonite particles: estimation of the clay edge sorption site density by low-pressure gas adsorption and AFM observations. *Am. Miner.* **88**, 1989–1995.

Tournassat, C., Greneche, J.M., Tisserand, D., Charlet, L., 2004a. The titration of clays minerals I. Disconstinuous backtitration technique combined to CEC measurements. *J. Colloid Interface Sci.* **273**, 228–237.

Tournassat, C., Ferrage, E., Poinsignon, C., Charlet, L., 2004b. The titration of clays minerals II. Structure-based model and implications for clay reactivity. *J. Colloid Interface Sci.* **273**, 238–250.

Van der Lee, J., De Windt, L., 2002. CHESS Tutorial and Cookbook. Updated for version 3.0. User Manual Nr. LHM/RD/02/13. Ecole des Mines de Paris, Fontainebleau, France.

Wanner, H., Albinson, Y., Karnland, O., Wieland, E., Wersin, P., Charlet, L., 1994. The acid/base chemistry of Montmorillonite. *Radiochim. Acta* **66/67**, 157–162.

Ward, D.B., Brady, P.V., 1998. Effect of Al and organic acids on the surface chemistry of kaolinite. *Clay. Clay Miner.* **46**, 453–465.

Wesolowski, D.J., Palmer, D.A., 1994. Aluminum speciation and equilibria in aqueous solution: V. Gibbsite solubility at 50 °C and pH 3–9 in 0.1 molal NaCl solutions (a general model for aluminum speciation; analytical methods). *Geochim. Cosmochim. Acta* **58**, 2947–2969.

Wieland, E., Stumm, W., 1992. Dissolution kinetics of kaolinite in acidic aqueous solutions at 25 °C. *Geochim. Cosmochim. Acta* **56**, 3357–3363.